AAC Accepts, published online ahead of print on 23 June 2014
Antimicrob. Agents Chemother. doi:10.1128/AAC.03389-14
Copyright © 2014, American Society for Microbiology. All Rights Reserved.

Synergy of streptogramin antibiotics occurs independently of their effects on translation

Jonas Noeske,[a] Jian Huang,[b] Nelson B. Olivier,[b] Robert A. Giacobbe,[c] Mark Zambrowski,[c] and Jamie H. D. Cate[a]#

Department of Molecular & Cell Biology, California Institute of Quantitative Biosciences, University of California, Berkeley, California, USA[a]; AstraZeneca R&D Boston, Discovery Sciences, Waltham, Massachusetts, USA[b]; AstraZeneca R&D Boston, Infection Innovative Medicines Unit, Waltham, Massachusetts, USA[c]

#Correspondence to Jamie H. D. Cate, jcate@lbl.gov

Running title: Streptogramin synergy and translation

AAC Accepts published online ahead of print

AAC Accepts published online ahead of print

16 ABSTRACT

17 Streptogramin antibiotics are divided into type A and B streptogramins, which in combination
18 can act synergistically. We compared the molecular interactions of the streptogramin
19 combinations Synercid (type A: dalfopristin, type B: quinupristin) and NXL 103 (type A:
20 flopristin, type B: linopristin) with the *Escherichia coli* 70S ribosome by x-ray crystallography.
21 We further analyzed the activity of the streptogramin components individually and in
22 combination. Streptogramin A and B components in Synercid and NXL 103 exhibit synergistic
23 antimicrobial activity against certain pathogenic bacteria. However, in transcription-coupled
24 translation assays, only combinations that include dalfopristin, the streptogramin A component
25 of Synercid, show synergy. Notably, the diethylaminoethylsulfonyl group in dalfopristin reduces
26 its activity, but is the basis for synergy in transcription-coupled translation assays before its rapid
27 hydrolysis from the depsipeptide core. Replacement of the diethylaminoethylsulfonyl group in
28 dalfopristin by a non-hydrolyzable group may therefore be beneficial for synergy. The absence
29 of general streptogramin synergy in transcription-coupled translation assays suggests that
30 synergistic antimicrobial activity of streptogramins can occur independently of streptogramin
31 effects on translation.

32

AAC Accepts published online ahead of print

INTRODUCTION

Bacterial infections caused by antibiotic resistant clinical isolates are an emerging medical threat. Based on conservative assumptions made by the Center for Disease Control (CDC), at least two million people acquire life-threatening infections caused by antibiotic resistant bacterial strains in the U.S. every year, resulting in 23,000 deaths. Despite the constant need for new antibiotics, the number of new antibiotics approved by the FDA has significantly decreased over the last decade (1, 2). Antibiotics that target the bacterial ribosome specifically interfere with key processes of protein synthesis such as mRNA decoding and peptide bond formation (3). The streptogramin antibiotics produced by some *Streptomycetes* strains inhibit protein synthesis by interfering with peptide bond formation and by blocking the peptide exit tunnel in the large (50S) ribosomal subunit, which prevents extension of the polypeptide chain (Fig. 1A). Streptogramin antibiotics are depsipeptides consisting of two chemically distinct types, a smaller type A, and a larger type B. Streptogramin antibiotics have been used as growth promoters in food-producing animals for over 50 years (4) but only began to be used to treat human infections with the approval of dalfopristin/quinupristin (Synercid), an injectable pair of streptogramin antibiotics (5) in 1999.

To counteract the spread of methicillin resistant *Staphylococcus aureus* (MRSA) in hospitals in the 1990s, Synercid was developed as a 70:30 (w/w) mixture of dalfopristin and quinupristin. Synercid was approved in 1999 for the treatment of life-threatening infections caused by vancomycin-resistant *Enterococcus faecium* (VREF) and complicated skin and skin structure infections (cSSSIs) caused by *S. aureus* or *Streptococcus pyogenes* and is currently the only clinically used streptogramin antibiotic. To overcome venous irritation caused by Synercid and in order to reduce health care costs, a new and orally available streptogramin combination

AAC Accepts published online ahead of print

flopristin/linopristin (NXL 103), a 70:30 (w/w) mixture of flopristin and linopristin, has been developed for use in the outpatient setting. NXL 103 has been shown to be more effective than Synercid in treating a large number of Gram-positive bacteria and their clinical isolates (6-9), and also has the potential to become an important drug in the treatment of community-acquired pneumonia and complex skin and soft tissue infections including MRSA (10).

Both streptogramin type A (dalfopristin and flopristin) and type B components (quinupristin and linopristin) differ between Synercid and NXL 103. The streptogramin A components dalfopristin of Synercid and flopristin of NXL 103 differ by a carbonyl oxygen at position 15 in dalfopristin which is replaced by a fluorine in flopristin. Furthermore, dalfopristin is derivatized on its pyrrolidine group with a diethylaminoethylsulfonyl group (Fig. 1B). Rapid hydrolysis of the dietylaminoethylsulfonyl group at physiological pH converts dalfopristin to viriginiamycin M (11). *In vitro* studies have shown that the streptogramin A flopristin in NXL 103 has higher antimicrobial activity than its counterpart dalfopristin in Synercid, suggesting that NXL 103's increased activity is mainly due to flopristin (6, 7). The streptogramin B component quinupristin of Synercid carries a quinuclidinylthiomethyl group, compared to a methylmorpholine group in linopristin of NXL 103 (Fig. 1B). Both quinupristin and linopristin are derived from virginiamycin S, which is not functionalized at its oxopiperidinyl group.

Streptogramins A and B must be used in combination, due to the fact that the individual streptogramin components exert a bacteriostatic effect, whereas their combination is bacteriocidal (12). Streptogramin A and B antibiotics act synergistically *in vitro* and in animal models of infection (13-15). Synergy between two antibiotics may be advantageous by reducing

AAC Accepts published online ahead of print

the likelihood of bacterial acquired resistance mutations of their binding site. Furthermore, in order to achieve a given bacteriocidal effect, smaller doses of the individual compounds are required, reducing potential side effects caused by the toxicity of the components. As opposed to experiments *in vivo* and *in vitro,* synergy has not been studied extensively in transcription-coupled translation assays with natural mRNAs. In cell-free translation assays using poly(U) directed polyphenylalanine synthesis, streptogramin A compounds showed activity, whereas streptogramin B compounds were inactive. However, streptogramin B antibiotics were active in inhibiting translation of poly(A,C) synthetic messages (16-18). In cell-free translation studies using cell extracts of the Gram-positive bacterium *Bacillus subtilis* infected with phage 2C, translation inhibition by a combination of virginiamycin M plus virginiamycin S was higher than the sum of the inhibitory effects of the individual virginiamycin components (19). Furthermore, in different studies, the binding affinity of streptogramin B was shown to increase in the presence of streptogramin A compared to streptogramin B alone (20, 21). However, these measurements were performed on purified ribosomes, which may not reflect the properties of actively translating ribosomes in intact cells or in transcription-coupled translation systems. Crystal structures of virginiamycin antibiotics bound to the large ribosomal subunit of the extreme halophilic archaeon *Haloarcula marismortui* and of Synercid to the extremophile *Deinococcus radiodurans* (22-24) reveal that nucleotide A2062 in 23S ribosomal RNA (rRNA), present in the binding pocket of both streptogramins, changes conformation upon streptogramin A binding only, which may explain the increased affinity for streptogramin B in the presence of streptogramin A.

AAC Accepts published online ahead of print

Here, we report the crystal structures of Synercid and NXL 103 as well as their individual components bound to the intact *Escherichia coli* 70S ribosome, which is more closely related to the ribosomes of pathogenic bacteria. Furthermore, we comprehensively tested the activity of individual streptogramin components in biochemical and microbiological assays, and for synergy between streptogramin A and B components. Antimicrobial assays were used to determine the minimal inhibitory concentration (MIC) of individual streptogramin antibiotics and "checkerboard" assays (25) were used to quantify the synergistic effect between the streptogramin A and B components. We also measured the activities of the individual streptogramin components as well as their combinations on protein synthesis in transcription-coupled translation extracts. Finally, we measured the affinity of streptogramin B to purified intact *E. coli* ribosomes either alone or in the presence of streptogramin A in order to investigate the synergistic effect at the molecular level.

MATERIALS & METHODS

Ribosome purification, ribosome crystallization, and antibiotic binding experiments

Ribosomes were purified from *E. coli* MRE600 cells as described previously (26). Crystals were grown from purified ribosomes as described previously (27). For antibiotic soaking experiments, ribosome crystals were soaked overnight in cryoprotection buffer supplemented with either pre-mixed Synercid (348 µM dalfopristin + 101 µM quinupristin), NXL 103 (120 µM flopristin + 70 µM linopristin), or with individual components (dalfopristin, quinupristin, flopristin, or linopristin) at a concentration of 100 µM. All components were dissolved in DMSO to a concentration of ~100 mM, except for premixed Synercid, which was dissolved in DMSO to a concentration of 348 mM dalfopristin and 101 mM quinupristin. DMSO

AAC Accepts published online ahead of print

stocks were diluted 1000-fold in cryoprotection buffer for soaking experiments, and crystals were flash frozen in liquid nitrogen for diffraction experiments. Pre-mixed Synercid (30% quinupristin and 70% dalfopristin, w/w) was a generous gift from Pfizer; flopristin and linopristin were provided by AstraZeneca; and dalfopristin and quinupristin were purchased from International Laboratory USA. Virginiamycin M1 was purchased from Sigma-Aldrich.

X-ray diffraction experiments and model building

X-ray diffraction data were measured at beamlines 8.3.1 and 12.3.1 at the Advanced Light Source, Lawrence Berkeley National Laboratory, and at beamline 11-1 at the Stanford Synchrotron Radiation Lightsource, SLAC National Accelerator Laboratory, with oscillation ranges of 0.2-0.3° at 100 K recorded on an ADSC Q315r detector or a Dectris PILATUS 6M detector. Diffraction data were reduced, scaled, and converted using the XDS Program Package (28). Difference electron density was calculated using the phenix.refine component of the PHENIX software suite (29). Antibiotics were modeled in the unbiased difference electron density obtained from each complex after molecular replacement. Changes to the rRNA structure were made using Coot (30), followed by individual atomic displacement parameter (ADP) refinement using phenix.refine. Restraint files for each antibiotic structure were generated using phenix.elbow of the PHENIX software suite.

Dalfopristin hydrolysis

DMSO stocks of dalfopristin and virginiamycin M_1 at 4 mM were dissolved in 0.01 M sodium phosphate buffer pH 7.4 or in cation adjusted Mueller Hinton II (CAMH II) media adjusted to pH 6.0 to yield a final concentration of 200 µM of target compound. Samples were

AAC Accepts published online ahead of print

prepared and monitored continuously for up to a 24-hour period at 37 ˚C. Hydrolysis of the target compounds was monitored via LC-MS SIM in ESI+ and ESI- mode. The natural log of the area responses for dalfopristin and virginiamycin M_1 were plotted against time and first order kinetics were used to derive the half-life ($t_{½}$) of each compound.

Prehydrolized dalfopristin for antimicrobial assays and transcription-coupled translation assays was prepared by dissolving dalfopristin to a concentration of 2.5 mM in 50 mM ammonium acetate, pH 7.5, containing 30% DMSO. Hydrolysis of dalfopristin was performed over 24 hours at 4 ˚C.

Antimicrobial Susceptibility Testing

The minimum inhibitory concentration (MIC) against each isolate was determined by broth microdilution technique in accordance with Clinical and Laboratory Standards Institute (CLSI) guidelines of document M07-A9, 2012 (31). Susceptibility breakpoint interpretations for reference compounds along with QC ranges for reference strains are described in CLSI, document M100-S23, 2013 (32). Following incubation, MIC values were determined visually and reported as the lowest concentration of drug that completely inhibited growth of the strain. A comparison of the streptogramins dalfopristin, quinupristin, flopristin, linopristin, hydrolyzed dalfopristin, and virginiamycin M was run versus five ATCC reference strains *E. coli* ATCC 29417 (MRE 600), *Enterococcus faecalis* ATCC 29212, *S. aureus* ATCC 29213, *Haemophilus influenzae* ATCC 49247, and *Streptococcus pneumoniae* ATCC 49619.

"Checkerboard" assay

AAC Accepts published online ahead of print

A checkerboard assay described by Pillai *et al. (33)* was used to determine the microbiological interaction with pairs of agents in a two-dimensional array. The MIC of streptogramin compounds (dalfopristin and quinupristin) and (flopristin and linopristin) alone or in combination were determined by the broth microdilution technique in accordance with Clinical and Laboratory Standards Institute guidelines of document CLSI, M07-A9, 2012 (31) against four ATCC cultures; *E. coli* ATCC 29417 (MRE600), *E. faecalis* ATCC 29212 and *S. aureus* ATCC 29213. By comparing the MIC of an agent alone to the MIC combination, a series of fractional inhibitory concentrations (FICs) can be calculated followed by FIC indices (34). MIC values were determined for each isolate against combinations of streptogramins. The agent combinations were measured as fold-reductions in MIC based on the original MIC. The FICs were calculated dividing the MIC of agent alone by the MIC of the agent when tested in combination. The FIC index was obtained by adding the FICs. The FIC indices were interpreted as synergistic when values were ≤ 0.5, additive/indifferent when values were > 0.5 to 4.0, and antagonistic when values were > 4.0. The following equation was used to calculate the FIC indices: $FIC_A + FIC_B$ = (MIC of [A] in Combo / MIC of A alone) + (MIC of [B] in Combo / MIC of B alone. A mean FIC index for synergic values was used to determine the possibility of drug interactions and interpretation of results according to accepted criteria (35).

Transcription-coupled translation assay

Plasmid pKK3535 containing the *rrnB* operon encoding for ribosomal RNA and a chloramphenicol resistance cassette was used for mutagenesis. U1782 and U2586 were mutagenized using the QuikChange kit from Agilent and the sequence of the entire operon was verified by sequencing. SCB 53 cells, in which all endogenous rRNA genes were deleted and

AAC Accepts published online ahead of print

194 replaced by a pKK3535 plasmid with an ampicillin resistance cassette (36), were transformed
195 with the mutagenized pKK3535 plasmid. Cells were first grown in liquid culture supplemented
196 with chloramphenicol and then plated on LB agar plates containing chloramphenicol. Successful
197 plasmid shuffling was confirmed by the absence of growth on a LB agar plate containing
198 ampicillin for single colonies picked from a LB agar plate supplemented with chloramphenicol.
199
200 Transcription-coupled translation assays were performed essentially according to
201 Buurman *et al.* (37). *E. coli* MRE600 cells were used to prepare wild type S30 cell extract as
202 described previously (37). Mutant *E. coli* S30 cell extract was prepared as wild type extract but
203 using an *E. coli* strain bearing a U1782C/U2586C double mutant. For the transcription-coupled
204 translation assay the following reagents were used. Reagent 1 consisted of 0.5 mM (each) ATP,
205 CTP, UTP, and GTP (Chem-Impex International, Wood Dale, IL), 20 mM phosphoenolpyruvate
206 (Chem-Impex International), 100 µg/ml *E. coli* tRNA (Roche Diagnostics Corp., Indianapolis,
207 IN), 20 µg/ml folinic acid, 1 mM cyclic AMP (cAMP), 0.8 mM isopropyl-β-d-
208 thiogalactopyranoside (IPTG), 0.2 mM DTT, 30 mg/ml polyethylene glycol 8000, 0.5 mM
209 (each) all 20 of the translated amino acids, 2 U/ml pyruvate kinase, and 40 µg/ml pLH1824
210 reporter plasmid DNA. Reagent 2 contained S30 extract prepared from either *E.coli* MRE600
211 strain (Paragon Bioservices, Baltimore, MD) or from a mutant *E. coli* strain as described above.
212 The S30 extract was diluted to 2 mg/ml in S30 buffer consisting of 10 mM Tris-acetate (pH 7.4),
213 60 mM potassium acetate, and 14 mM magnesium acetate. Both reagents were allowed to
214 preincubate at room temperature for 1 hour.
215

AAC Accepts published online ahead of print

To determine IC50 values of the streptogramins, the compounds were dissolved in DMSO to 2.5 mM and 2-fold serially diluted in DMSO. Hydrolyzed dalfopristin was dissolved in hydrolyzing buffer (see dalfopristin hydrolysis section) and serially diluted in DMSO. Diluted compound (0.3 µL) was added to 384-well white polystyrene assay plates (Corning, Inc., Lowell, MA) using the Bravo Automated Liquid Handling Platform (Agilent Technologies, Santa Clara, CA). To determine additive/synergistic effects between class A and B streptogramins, two experiments were carried out. In the first experiment, the effect of streptogramin B on the activity of streptogramin A was determined. Class A streptogramins were serially diluted and added to the assay plate using the Bravo Platform as described above. Subsequently, class B streptogramins, dissolved in DMSO, were added to the assay plate using the Echo Liquid Handler (Labcyte Inc. Sunnyvale, CA) to yield a final concentration in the reaction equal to their respective IC50 values. In a second experiment, the effect of streptogramin A on the activity of streptogramin B was determined. Class A compounds were added to the assay plates using the Bravo Platform to yield a concentration of their respective IC50 values in the final reaction. In a second step, serially diluted class B compounds (0.3 µL) were added to the assay plate using the Echo Liquid handler. Therefore, in the first experiment the Bravo Platform was used to deliver a serial dilution of the streptogramin A compound whereas in the second experiment the same platform was used to deliver the streptogramin A compound fixed at its IC50. For percent inhibition calculations, luminescence intensity from the samples receiving maximum dose of compounds were referenced as 100% inhibition, and the samples with minimum dose of compounds were referenced as 0% inhibition. Mean IC50 values from a representative experiment performed in triplicate are shown with standard deviation.

AAC Accepts published online ahead of print

After streptogramin compounds were added to the assay plate reagent 1 (15 µL) was added, followed by 15 µL of reagent 2. The plate was then briefly shaken in an Eppendorf Mixmate plate shaker. The plates were sealed with foil and incubated at room temperature for 30 minutes, avoiding temperature fluctuation. Subsequently, 15 µL of luciferin developer consisting of 0.4 µM lithium salt of coenzyme A (Sigma), 0.7 µM D-luciferin (Gold Biotechnology, St. Louis MO), 0.8 µM ATP, 20 mM Tricine (pH 7.8), 1 mM magnesium carbonate, 0.1 mM EDTA, 2.3 mM magnesium sulfate, and 33 mM DTT was added, and light production was measured immediately using a Pherastar plate reader (BMG Labtech, Ortenberg, Germany).

Isothermal titration calorimetry

Isothermal titration calorimetry was performed in a MicroCal Auto-iTC200 System (GE Healthcare). Purified *E. coli* 70S ribosomes were dialyzed against 20 mM Tris HCl pH 7.5, 60 mM NH_4Cl, 6 mM $MgCl_2$, 0.5 mM EDTA, and 2 mM TCEP at 4 ˚C either without or in the presence of 1.5 equivalent dalfopristin or flopristin in the dialysis buffer. Quinupristin or linopristin (39 µM) dissolved in dialysis buffer was titrated into the cell containing 2.2 - 3.9 µM 70S ribosome either alone or in the presence of either dalfopristin or flopristin with a first injection of 0.5 µl volume followed by 12 injections of 3.1 µL volume at 4 ˚C.

RESULTS

NXL 103 has been shown to be more potent compared to Synercid against a variety of Gram-positive pathogens and against *H. influenzae* (8, 38). In order to shed light on the increased activity of NXL 103 versus Synercid we solved crystal structures of the 70S *E. coli* ribosome in complex with either Synercid or NXL 103 or their individual components at 2.8 - 3.0 Å

AAC Accepts published online ahead of print

resolution (Table S1). Positive difference electron density was observed in an unbiased F_{obs}–F_{calc} map for both streptogramin A and B components. The chemical structures of streptogramin A and B were modeled into the electron density, thereby unambiguously identifying their location, orientation, and conformation (Fig. 1C,D, Fig. S1).

Binding mode of Synercid

Dalfopristin binds to the large ribosomal subunit at the entrance of the exit tunnel to a hydrophobic pocket (Fig. 1A). The macro lactone ring stacks under the bases of G2061 and A2451, thereby forming favorable hydrophobic interactions between its aliphatic stretch (C9 to C12) and the base of G2061, and between its oxazole group and the base of A2451. Upon binding of the streptogramin pair, the base of A2062 moves towards the streptogramin A molecule to form stacking interactions with both streptogramin A and B (Fig. 1C). As a result, the amide bond of dalfopristin stacks on the base of A2062. The streptogramin-induced movement of A2062 positions the 2'-OH group of A2062 to form a hydrogen bond with the amide oxygen of dalfopristin (Fig. 1C). Furthermore, the carbonyl oxygen of C6 and C26 each form a hydrogen bond with the exocyclic amino group of G2061, and the only hydroxyl group of dalfopristin forms a hydrogen bond with the non-bridging phosphate oxygen of G2505. The structure reveals that acetylation of the C13 hydroxyl group, a known resistance mechanism (39) would interfere with dalfopristin binding by steric hindrance.

Quinupristin, the streptogramin B component of Synercid, binds to the large ribosomal subunit at the entrance of the exit tunnel adjacent to dalfopristin (Fig. 1A,C). The hydroxypicoline group of quinupristin stacks on the opposite face of the base of A2062

AAC Accepts published online ahead of print

compared to dalfopristin. This positions the base of A2062 to form two hydrogen bonds with quinupristin, between the N1 and N6 of A2062 and the N16 amide nitrogen and the C14 carbonyl oxygen of quinupristin, respectively (Fig. 1C). These contacts and favorable stacking interactions are likely disrupted by an A2062C mutation found in *S. pneumoniae*, which confers resistance to streptogramins and macrolides (40). Quinupristin stacks with its aliphatic stretch comprising atoms C17 to C19 including its C19 methyl group on the base of U2586 and also with its phenyl group under the ribose of U2609. The dimethylaminophenyl group of quinupristin stacks on the edge of A2058. This hydrophobic interaction is likely crucial for streptogramin B binding since A2058 N6 methylation by *erm* methyltransferases and mutation of A2058 to either G, U, or C leads to streptogramin B resistant phenotypes in *Helicobacter pylori* (41) and *E. coli* (42).

Binding of Synercid to the large ribosomal subunit causes dramatic structural rearrangements in the peptidyl transferase center (PTC). In the vacant E. coli ribosome, the base of U2585 reaches into the entrance of the exit tunnel to a position that is occupied by the lactone group of dalfopristin when Synercid is bound. Binding of Synercid causes nucleotide U2585 to flip by 160º away from the peptidyl transferase center. In this alternate conformation, the O4 of U2585 coordinates a magnesium ion, which in turn coordinates one non-bridging phosphate oxygen of each of the two proceeding residues, U2584 and G2583 (Fig. 1E). This magnesium ion, not present in the vacant ribosome structure, and the base flip of U2585 force the G2583:U2506 wobble base pair to break and nucleotide U2506 to move out of the plane of the G:U base pair. Although the archaeal *H. marismortui* 50S ribosomal subunit and *E. coli* 70S ribosome structures differ in the positioning of A2503 in the exit tunnel, when either

AAC Accepts published online ahead of print

virginiamycin M or both virginiamycin M and virginiamycin S are bound, A2503 and A2062 assume identical positions in the *H. marismortui* 50S subunit (22, 24), compared to their positions observed in the *E. coli* ribosome bound to Synercid.

Binding mode of NXL 103

Flopristin binds to the same site as dalfopristin and adopts similar hydrophobic interactions and hydrogen-bonding patterns with the ribosome. Flopristin differs from dalfopristin by a fluorine atom bonded to an sp^3 hybridized C15 carbon, which is a carbonyl group in dalfopristin. Neither the carbonyl of dalfopristin nor the fluorine of flopristin are within hydrogen-bonding distance of ribosomal components. Despite the highly similar binding modes of dalfopristin and flopristin, the absence of the diethylaminoethylsulfonyl group in flopristin (Fig. 1B) has a dramatic effect on the conformation of the peptidyltransferase center (PTC). Unlike the binding of Synercid, NXL 103 causes nucleotide U2585 to flip only by about 45° and its base to rotate by ~90° compared to the vacant 70S ribosome structure (Fig. 1E). This conformational change causes the G2583:U2506 wobble base pair to break. U2506 flips out of the plane of the G:U wobble base pair and clamps together U2583-G2585 by an intricate network of hydrogen bonds, thereby stabilizing this alternate conformation of the PTC (Fig. 1F). Interestingly, if the complex of dalfopristin bound to the *E. coli* 70S is crystallized under conditions that favor hydrolysis of the diethylaminoethylsulfonyl group, U2585, U2584, and G2583 together with their base pairing partners assume a conformation identical to that seen in the complex with flopristin (Fig. 1E).

AAC Accepts published online ahead of print

Linopristin, the streptogramin B component of NXL 103, binds to the same site as its counterpart quinupristin of Synercid and maintains all of the hydrophobic interactions and hydrogen bonding interactions with A2062. Linopristin differs from quinupristin by the replacement of the quinuclidinylthiomethyl group in quinupristin with a methylmorpholine group in linopristin (Fig. 1B). The morpholine of linopristin does not penetrate the exit tunnel as far as the qinuclidinyl group of dalfopristin, and forms a hydrogen bond to the ε-amino group of lysine 90 in ribosomal protein L22, which in turn forms an additional hydrogen bond with a non-bridging phosphate oxygen of U747. In the vacant ribosome structure, K90 forms a salt bridge with a non-bridging phosphate oxygen of U747 and in the quinupristin structure, the quinuclidinyl group displaces the side chain of K90 thereby disrupts its interaction with U747 (Fig. 1G). Interestingly, when linopristin alone is bound to the ribosome the morpholine group no longer forms a hydrogen bond to K90 and furthermore A2058 and A2059 move apart by 1Å. Linopristin's dimethylaminophenyl group moves over the newly formed gap and no longer stacks on the edge of A2058 (Fig. S2). This suggests that linopristin’s binding mode shifts due to the presence of the streptogramin A component.

The structures of Synercid and NXL 103 and their individual components (except for linopristin alone) reported here superimpose within the limits of coordinate error with viginiamycin M + S bound to the *H. marismortui* 50S ribosomal subunit (22, 24), whereas the present structures differ from those reported for Synercid bound to the *D. radiodurans* 50S ribosomal subunit (23). For example, the macrolactone rings of both the streptogramin A and B components in the *D. radiodurans* 50S subunit are shifted to different extents with respect to their counterparts in the structures reported here and in the *H. marismortui* 50S subunit

AAC Accepts published online ahead of print

353 structures. In the *D. radiodurans* 50S subunit, both the pyrrolidine as well as the oxazole group
354 of the streptogramin A component are displaced compared to their counterparts in the *E. coli* and
355 *H. marismortui* structures. Further, A2062 assumes a different conformation in the *D.*
356 *radiodurans* context and therefore fails to stack on the amide group of streptogramin A and the
357 hydroxypicoline group of streptogramin B. Finally, the dalfopristin specific
358 diethylaminoethylsulonyl group and U2585 in the *D. radiodurans* structure assume different
359 conformations compared to the structure of Synercid bound to the *E. coli* 70S ribosome. The
360 observed differences between the Synercid structures of *E. coli* and *D. radiodurans* could be due
361 to the fact that the ribosomes are from divergent bacterial species or due to the low resolution of
362 the *D. radiodurans* structure (3.4 Å) compared to the present structures (Table S1). Given the
363 similarity of the present *E. coli* structures with those with the *H. marismortui* 50S subunit, the
364 binding mode of Synercid and the associated conformational changes in the ribosome observed
365 here probably reflect the relevant structures for understanding streptogramin interactions with
366 ribosomes in pathogenic bacteria.
367
368 **Dalfopristin hydrolysis**
369 Dalfopristin has been reported to hydrolyze rapidly to virginiamycin M under
370 physiological conditions (11). In order to estimate the effects of dalfopristin hydrolysis on its
371 potency, we first determined the hydrolysis rate of dalfopristin at pH 7.4 and pH 6.0 using mass
372 spectrometry (Fig. S4). Dalfopristin hydrolyzes to virginiamycin M with a half-life ($t_{1/2}$) of
373 about 11 min at pH 7.4 and 77 min at pH 6.0. The hydrolysis product virginiamycin M is very
374 stable at pH 7.4 with a half-life of about 45 hr. The antimicrobial assays performed in this study
375 ran over the course of 16-24 hr, thus the effect of dalfopristin in these experiments can be

AAC Accepts published online ahead of print

376 attributed to its hydrolysis product virginiamycin M. Transcription-coupled translation assays
377 lasted 30 min at pH 7.5 and therefore substantial hydrolysis of dalfopristin will have occurred.
378 However, due to the shorter time frame of the transcription-coupled translation assays the
379 activity of dalfopristin can in part be attributed to its unhydrolyzed form.
380
381 **Antimicrobial activities of streptogramin antibiotics**
382 In order to determine the antimicrobial activities of streptogramin antibiotics on living
383 cells, minimal inhibitory concentrations (MIC) were determined by growing different Gram-
384 positive and Gram-negative pathogens in the presence of different concentrations of
385 streptogramin antibiotics. MICs for streptogramin antibiotics were generally in the low µg/mL
386 range, with the exception of streptogramin B in Gram-negative species and streptogramin A in *E.*
387 *faecalis*. The streptogramin B antibiotics quinupristin and linopristin had very little to no effect
388 on growth of the Gram-negative pathogens *E. coli* and *H. influenzae* which is likely due to the
389 inability of these antibiotics to permeate the outer cell membrane and is in agreement with
390 previous results (43). *E. faecalis* showed MICs of 64 µg/mL towards streptogramin A antibiotics,
391 likely due to its *lsa* gene, which encodes for a putative ABC transporter leading to streptogramin
392 A efflux (44). In all other bacterial strains tested, flopristin showed higher activity compared to
393 dalfopristin, and linopristin showed equal or lower activity than quinupristin (Table 1). For all
394 strains, MIC values for dalfopristin administered in its prehydrolyzed form were within two-fold
395 of MIC values of virginiamycin M, which is chemically identical to dalfopristin's hydrolysis
396 product.
397

AAC Accepts published online ahead of print

We also used a "checkerboard" assay to evaluate synergy of Synercid and NXL 103 in *E. coli*, *E. faecalis*, and *S. aureus*. The streptogramin components of Synercid and NXL 103 did not show a synergistic mode of action in *E. coli.* This finding is expected since individually quinupristin and linopristin did not affect bacterial growth even at the highest concentrations tested (Table 1). A synergistic mode of action was observed for Synercid and NXL 103 in *E. faecalis* with a lower mean fractional inhibitory concentration (FIC) index for NXL 103 compared to Synercid (Table 2). For Synercid synergy was observed at three different concentration pairs whereas for NXL 103 synergy was observed for six different concentration pairs (Table 2). In *S. aureus* greater synergy was observed for both Synercid and NXL 103 compared to *E. faecalis* as judged by their lower mean FIC index for all combinations that led to synergy. Furthermore, in *S. aureus,* synergy occurred at lower streptogramin concentrations compared to *E. faecalis* for both Synercid and NXL 103 (Table 2). Taken together these results show that NXL 103 generally exhibits a higher degree of synergy than Synercid in the context of a given bacterial strain.

Effects of streptogramin antibiotics in transcription-coupled translation assays

We used an *E. coli* based transcription-coupled translation assay to determine the inhibitory effects of streptogramin antibiotics on actively translating ribosomes. Although the translation assay employed cell extracts from the Gram-negative *E. coli* and Synercid is indicated for the Gram-positive pathogens *S. aureus* and *S. pyogenes,* only one major sequence difference occurs for residues within a radius of 10 Å of the ribosomal binding sites of both streptogramins in a range of Gram-negative and Gram-positive pathogens (Fig. 2A, Fig. S5). In many Gram-negative pathogenic bacteria, including *E. coli,* the streptogramin B binding pocket includes a U-

AAC Accepts published online ahead of print

U base pair at position 1782-2586 whereas this base pair is a C-C base pair in many Gram-positive pathogenic bacteria including *S. aureus* and *S. pyogenes* (Fig. 2A). Apart from this difference, changes further away from the binding pockets include unpaired U1781, which is found to be a G in *B. subtilis*, *Bacillus anthracis*, and *Listeria monocytogenes* and a C in *Clostridium difficile* and *Propionibacterium avidum*, and three canonical W-C base pairs (744-753, 2070-2441, 2067-2443) that are different canonical WC base pairs in different pathogens (Fig. S5). However, all these changes are located in the second or third shell of the binding site and do not immediately constitute the streptogramin binding pocket. Notably, the crystal structure of the *H. marismortui* 50S reveals that a G at position 1781 does not change the geometry of the U1782-U2586 base pair (45). From this alignment we conclude that the only difference between Gram-negative and Gram-positive pathogens and more specifically between *E. coli* and *S. aureus* / *S. pyogenes* that could impact streptogramin activity is the U1782C/U2586C double mutation in the streptogramin B binding site (Fig. S6). In order to account for the rRNA sequence differences between Gram-positive and Gram-negative pathogens, a mutant *E. coli* strain was constructed containing a C1782-C2586 base pair instead of a U-U base pair in the streptogramin B binding pocket to prepare a transcription-coupled translation extract.

We measured the concentration of the individual streptogramin A and B components that cause 50% inhibition of translation (IC50) in transcription-coupled translation assays in the context of wild type (U-U) and the mutant (C-C) streptogramin binding pockets. Wild type and mutant *E. coli* TT assays were performed with the streptogramin B compounds linopristin and quinupristin, and the streptogramin A compounds flopristin, unhydrolyzed dalfopristin,

AAC Accepts published online ahead of print

444 virginiamycin M, and prehydrolyzed dalfopristin. Flopristin has an IC50 value of 130 nM and is
445 the compound with the highest activity in wild type TT assays (Fig. 2B, Table S2). Notably,
446 dalfopristin preincubated in buffer at pH 7.5 and therefore hydrolyzed to virginiamycin M has an
447 IC50 of 192 nM, nearly identical to authentic virginiamycin M (IC50 of 182 nM), as expected.
448 By contrast, unhydrolyzed dalfopristin is about 2.6-fold less active than hydrolyzed dalfopristin
449 (Fig. 2B, Table S2). This indicates that the diethylaminoethylsulfonyl group in dalfopristin is
450 detrimental for activity. The activity of all streptogramin A antibiotics were also tested in the
451 context of the Gram-positive streptogramin-binding site using the mutant (C-C) cell extract. The
452 mutant extract yielded comparable activities to wild type *E. coli* extract indicating that the
453 U1782C/U2586C double mutation does not affect streptogramin A activity. By contrast, the
454 activity of linopristin increased 1.9-fold in the mutant (C-C) extract compared to the wild type
455 (U-U) extract and quinupristin's activity increased 1.5-fold. Interestingly, linopristin and
456 quinopristin have more similar activities to each other in the C-C extract compared to the U-U
457 extract (Fig. 2B, Table S2).
458
459 To test whether streptogramin antibiotics have synergistic activity on ribosomes
460 translating a natural mRNA in a transcription-coupled translation assay, we determined the IC50
461 values of the streptogramin A antibiotics in the presence of a streptogramin B antibiotic at its
462 IC50 and vice versa, using a luciferase reporter mRNA. The IC50 of flopristin and
463 viriginiamycin M in the presence of either quinupristin or linopristin at their respective IC50
464 values decrease only marginally in the wild type (U-U) extract. By contrast, the IC50 of non-
465 hydrolyzed dalfopristin decreases substantially in the presence of quinupristin or linopristin at
466 their IC50 values (Fig. 2C, Table S3), representing an increase in dalfopristin activity up to 3.7-

AAC Accepts published online ahead of print

467 fold in the presence of linopristin. In the context of the Gram-positive (C-C) streptogramin-
468 binding site, the activity change of either flopristin or virginiamycin M in the presence of either
469 of the streptogramin B compounds is negligible (Fig. 2D, Table S3). Furthermore, in the context
470 of the Gram-positive streptogramin-binding site, dalfopristin potency increases only 1.6-fold in
471 the presence of linopristin and only 1.2-fold in the presence of quinupristin at their respective
472 IC50 values, a substantially less pronounced effect than in the Gram-negative system (Fig. 2C,D,
473 Table S3).
474
475 In the converse experiments, we held the streptogramin A component at its IC50
476 concentration and varied the concentration of the streptogramin B component. In the context of
477 the U-U streptogramin B binding site the IC50 of either linopristin or quinupristin in the
478 presence of flopristin or virginianycin M remains unchanged compared to the IC50 of the
479 respective streptogramin B antibiotic alone (Fig. 2E,F, Table S4). By contrast, the IC50 of
480 linopristin decreased 4.5-fold in the presence of unhydrolyzed dalfopristin at its IC50 (Fig. 2E,
481 Table S4). Furthermore, the IC50 of the other streptogramin B, quinupristin, decreased only 2.1-
482 fold in the presence of unhydrolyzed dalfopristin at its IC50 (Fig. 2F, Table S4). In the context of
483 the C-C streptogramin-binding site, the IC50 values of linopristin (Fig. 2G, Table S4) and
484 quinupristin (Fig. 2H, Table S4) alone remained unchanged compared to their IC50 values in the
485 presence of either flopristin or viriginiamycin M. The IC50 of both linopristin and quinupristin
486 decreased in the presence of unhydrolyzed dalfopristin at its IC50 in the context of the C-C
487 streptogramin binding site, but the decreases were less pronounced compared to those observed
488 with the U-U streptogramin binding site (Fig. 2G,H versus 2E,F, Table S4). We also analyzed
489 the effects of prehydrolyzed dalfopristin alone, which is chemically equivalent to virginiamycin

AAC Accepts published online ahead of print

490 M and in combination with either of the two streptogramin B components, quinupristin and
491 linopristin. The results show that prehydrolyzed dalfopristin behaves similarly to virginiamycin
492 M, with slight differences likely due to differences in the antibiotic stock solution compositions
493 (see Methods).
494
495 Taken together, these results reveal that neither streptogramin A compounds flopristin
496 and virginiamycin M nor the streptogramin B compounds quinupristin and linopristin influence
497 their respective IC50 values in either the Gram-negative or Gram-positive streptogramin-binding
498 site contexts. However, the IC50 of dalfopristin is significantly lower in the presence of either
499 linopristin or quinupristin than by itself, especially in the context of the Gram-negative (U-U)
500 streptogramin binding site (Fig. 2C,D, Table S3). The IC50 values of linopristin and quinupristin
501 also drop in the presence of dalfopristin (Fig. 2E,F, Table S4). The effects in the context of the
502 Gram-positive (C-C) streptogramin-binding site are not as strong but are still observed (Fig.
503 2G,H, Table S4). Dalfopristin and virginiamycin M are chemically identical except for the
504 presence of the additional sulfonyl group in dalfopristin. The results shown here indicate that this
505 bulky sulfonyl group in dalfopristin is detrimental to dalfopristin activity as evident by the
506 reduced activity of dalfopristin compared to virginiamycin M. However, the sulfonyl group leads
507 to some degree of synergy between dalfopristin in the presence of a streptogramin B component
508 on actively translating ribosomes.
509
510 **Binding affinities of streptogramin antibiotics to vacant 70S ribosomes**
511 We also investigated whether the dissociation constant of streptogramin B to the isolated
512 *E. coli* vacant 70S ribosome is affected in the presence of saturating concentrations of

AAC Accepts published online ahead of print

streptogramin A. We determined the dissociation constant of either quinupristin or linopristin alone or in the presence of dalfopristin or flopristin, respectively, using isothermal titration calorimetry (ITC). Quinupristin alone binds to the 70S ribosome with a K_d of 44 ± 21 nM, and its affinity for the ribosome increases about six-fold in the presence of dalfopristin (Table 3, Fig. S7 and Table S5). In these experiments, performed at pH 7.5, dalfopristin was present in its hydrolyzed form. Similarly, the affinity of linopristin for the ribosome increases over three-fold when the ribosome was preincubated with flopristin (Table 3, Fig. S7 and Table S5). These results show that the affinity of the streptogramin B component increases in the presence of the streptogramin A component, as observed previously (20, 21). Crystallographic structures of the complexes of either dalfopristin or flopristin alone bound to the *E. coli* ribosome reveal that the base of A2062 has already moved by 2Å to stack on the amide of the streptogramin A component and that subsequent binding of streptogramin B only results in a small shift of A2062 in the plane of its nucleobase to maximize stacking interactions (Fig. S3). Since large areas of the streptogramin B component do not interact with the ribosome directly, pre-positioning of A2062 due to streptogramin A binding likely leads to a better defined and more rigid binding pocket for subsequent streptogramin B binding (22, 24).

DISCUSSION

Here, we assessed the activities of streptogramin combinations as well as their individual components in a transcription-coupled translation assay and determined the binding mode of both streptogramin combinations in a common system, the Gram-negative *E. coli* ribosome. Prior studies demonstrated that NXL 103 displays higher antimicrobial activity compared to Synercid and further showed that flopristin, the individual streptogramin A component of NXL

AAC Accepts published online ahead of print

103, showed higher activity than the corresponding streptogramin A in Synercid – dalfopristin. By contrast, the activity of linopristin, the streptogramin B component of NXL 103, showed varying activities compared to quinupristin, the corresponding streptogramin B in Synercid. From these studies it was concluded that higher activity of NXL 103 versus Synercid is based on its streptogramin A component flopristin (6-9, 38). Our antimicrobial and biochemical investigations confirm that flopristin is consistently more active than virginiamycin M or pre-hydrolyzed dalfopristin whereas linopristin either displays similar or reduced activity compared to quinupristin.

The rapid hydrolysis of the diethylaminoethylsulfonyl group in dalfopristin to virginiamycin M at physiological pH, with a half-life of 11 min, indicates that this group is not the basis for dalfopristin's decreased antimicrobial activity compared to flopristin, due to the duration of the experiment. However, our studies reveal that hydrolyzed dalfopristin or virginiamycin M bound to the ribosome is structurally essentially identical to flopristin and that neither the fluorine in flopristin nor the carbonyl group present in hydrolyzed dalfopristin are positioned in a way to interact with the ribosome. Thus, differences in biochemical and antimicrobial activity of flopristin (Fig. 2, Tables 1 and S1) compared to virginiamycin M are not structurally observable, but likely depend on energetic and kinetic parameters of translation.

Since Synercid is used to treat infections caused by Gram-positive species, we investigated differences in the constitution of both streptogramin A and B binding pockets of the Gram-negative *E. coli* compared to those of pathogens treated by Synercid as well as *B. subtilis*. The sequence alignment of all 23S rRNA residues within 10Å of the bound streptogramin

AAC Accepts published online ahead of print

559 components reveals one major difference: in Gram-negative pathogens a U-U base pair is found
560 at position 1782-2586 whereas it is a C-C base pair in most Gram-positive pathogens. This
561 indicates that a U1782C/U2586C double mutation in the *E. coli* system would mimic a Gram-
562 positive-like system in terms of its streptogramin binding site. While the activities of
563 streptogramin A components are identical in wild type compared to mutant translation extracts,
564 the activities of linopristin and quinupristin increased in the context of the Gram-positive versus
565 the Gram-negative binding site. The increased activity of streptogramin B components seems
566 surprising at first since the base pairing geometry and the hydrogen bonding pattern in a C-C
567 base pair is retained with respect to a U-U base pair (Fig. S8). However, more favorable dipole-
568 dipole interactions between the streptogramin B component and the C-C base pair compared to a
569 U-U base pair may rationalize the observed increased activity of streptogramin B components to
570 ribosomes with a C-C pair at position 1782-2586 (46). The streptogramin B component positions
571 its amide group at position 17 directly under the nucleobase of nucleotide 2586. This amide
572 group has a dipole moment that is positioned at about 50˚ with respect to the dipole moment of
573 the uracil base of 2586. However, a cytosine base at position 2586 results in dipole moment at
574 about 130˚ with respect to the dipole moment of the streptogramin B amide group. Further,
575 cytosine bases have a larger dipole moment compared to uracil bases (Fig. S8) (46), which
576 further favors positive attractions between the streptogramin B component and a cytidine at
577 2586. These findings may explain the increased activity of streptogramin B components
578 observed in transcription-coupled translation assays utilizing cell extract from an *E. coli* strain
579 bearing a C-C base pair at position 1782-2586 that mimics the streptogramin-binding site in
580 Gram-positive pathogens.
581

AAC Accepts published online ahead of print

582 Streptogramin antibiotics are known for their synergistic mode of action, as *in vitro* and
583 *in vivo* studies revealed that the activity of the streptogramin combination exceeds the sum of the
584 activities of the individual components (13-15). Our *in vitro* studies showed the synergistic effect
585 of NXL 103 and Synercid in Gram-positive pathogens (Table 1), with a higher degree of synergy
586 for NXL 103 versus Synercid in *S. aureus* and *E. faecalis*, as judged by their mean FIC indices
587 (Table 2). Increased binding affinities of streptogramin B in the presence of streptogramin A
588 compared to streptogramin B alone was previously suggested to confer the synergistic effect on a
589 molecular level (20, 21). However, these studies used purified empty ribosomes, which may not
590 reflect actively translating ribosomes. Furthermore, the binding affinity of antibiotics to their
591 target may not be directly correlated to their activity.
592
593 Only one study has been published that demonstrated some degree of synergy for the
594 combination of virginiamycin M and virginiamycin S using a translation system derived from *B.*
595 *subtilis* (19). Using transcription-coupled translation assays with cell extract from either a wild
596 type *E. coli* strain or an *E. coli* mutant strain bearing the U1782C/U2586C double mutant, we
597 found that no synergy occurs for any streptogramin combination in either extract with the
598 exception of combinations that include dalfopristin. Therefore, since no general synergistic
599 effects could be observed in either U-U or C-C based transcription-coupled translation systems,
600 but could be observed in antimicrobial assays, the synergistic effect of streptogramin
601 components likely occurs independent of protein synthesis. Future experiments will be required
602 to dissect the basis for streptogramin synergy in cells.
603

AAC Accepts published online ahead of print

In translation extracts, the only synergy that we were able to observe occurred with streptogramin combinations in which one of the components is dalfopristin containing its diethylaminoethylsulfonyl group. However, the diethylaminoethylsulfonyl group reduces dalfopristin's activity by at least 2.8 fold compared to virginiamycin M, dalfopristin's hydrolysis product. As the transcription-coupled translation assay is run at pH 7.4 for 30 min, during which time extensive hydrolysis of dalfopristin will have occurred, it is likely that the activity for completely unhydrolyzed dalfopristin is even lower. Thus, while the detrimental effect of the diethylaminoethylsulfonyl group of dalfopristin can be overcome in the presence of a streptogramin B compound by synergy, it will likely be necessary to employ an analogue of dalfopristin with a non-hydrolyzable group instead of the diethylaminoethylsulfonyl group, so long as the size of this added group does not severely impact dalfopristin activity.

PDB ACCESSION CODES

Coordinates and structure factors for 70S ribosomes bound to streptogramin antibiotics were deposited in the Protein Data Bank. There are four entries for each complex. The electron density maps of the first ribosomes are better than of the second ribosome in the asymmetric unit. Therefore, entries for the subunits of the first ribosome are of better quality than those of the second ribosome. Dalfopristin and quinupristin (Synercid) (4TP8, 4TP9, 4TPA, 4TPB), flopristin and linopristin (NXL 103) (4TPC, 4TPD, 4TPE, 4TPF), flopristin (4TOU, 4TOV, 4TOW, 4TOX), linopristin (4TOL, 4TOM, 4TON, 4TOO), dalfopristin (4TP0, 4TP1, 4TP2, 4TP3), quinupristin (4PE9, 4PEB, 4PEA, 4PEC), dalfopristin under hydrolyzing conditions, which is chemically equivalent to virginiamycin M (4TP4, 4TP5, 4TP6, 4TP7).

AAC Accepts published online ahead of print

627 ACKNOWLEDGEMENT

628 We thank R. Wilson for technical assistance with isothermal titration calorimetry
629 experiments and G. Meigs and J. Holton for assistance at beam line 8.3.1 at the Advanced Light
630 Source (ALS) and T. Doukov for assistance at beam line 11-1 at the Stanford Synchrotron
631 Radiation Laboratory (SSRL). We thank S. Blanchard (Weill Cornell Medical College) for
632 providing the pKK3535 ribosome plasmid and *E. coli* strain SCB 53. We also acknowledge
633 helpful discussions by members of the Cate laboratory and we acknowledge S. Mills' assistance
634 and consult in establishing a productive collaboration between UC Berkeley and AstraZeneca.

635 This work was supported by NIH grant R01-GM65050 to J.H.D.C., by the NIH project
636 MINOS grant R01GM105404 for the Structural Integrated Biology for Life Sciences (SIBYLS)
637 and 8.3.1 beam lines at the ALS, and by the U.S. Department of Energy (DEAC02-05CH11231
638 for the SIBYLS and 8.3.1 beamlines at the ALS). J. N. was funded by a Human Frontiers in
639 Science Program Long-Term Postdoctoral Fellowship.

640

641 REFERENCES

642 1. **Center for Disease Control and Prevention**. 2013. Antibioitic Resistance Threats in the
643 United States. Threat Report 2013.

644 2. **Donadio S, Maffioli S, Monciardini P, Sosio M, Jabes D.** 2010. Antibiotic discovery in
645 the twenty-first century: current trends and future perspectives. J. Antibiot. (Tokyo)
646 **63:**423-430.

647 3. **Wilson DN.** 2014. Ribosome-targeting antibiotics and mechanisms of bacterial
648 resistance. Nat. Rev. Microbiol. **12:**35-48.

AAC Accepts published online ahead of print

649 4. **Yates JD, Schaible PJ.** 1962. Virginiamycin as an antibiotic for poultry feeds. Nature
650 **194:**183-184.

651 5. **Pfizer.** 2013. Synercid® I.V. (quinupristin and dalfopristin for injection), Pfizer
652 Products.

653 6. **Dupuis M, Leclercq R.** 2006. Activity of a new oral streptogramin, XRP2868, against
654 gram-positive cocci harboring various mechanisms of resistance to streptogramins.
655 Antimicrob. Agents Chemother. **50:**237-242.

656 7. **Eliopoulos GM, Ferraro MJ, Wennersten CB, Moellering RC, Jr.** 2005. In vitro
657 activity of an oral streptogramin antimicrobial, XRP2868, against gram-positive bacteria.
658 Antimicrob. Agents Chemother. **49:**3034-3039.

659 8. **Goldstein EJ, Citron DM, Merriam CV, Warren YA, Tyrrell KL, Fernandez HT,**
660 **Bryskier A.** 2005. Comparative in vitro activities of XRP 2868, pristinamycin,
661 quinupristin-dalfopristin, vancomycin, daptomycin, linezolid, clarithromycin,
662 telithromycin, clindamycin, and ampicillin against anaerobic gram-positive species,
663 actinomycetes, and lactobacilli. Antimicrob. Agents Chemother. **49:**408-413.

664 9. **Mabe S, Champney WS.** 2005. A comparison of a new oral streptogramin XRP 2868
665 with quinupristin-dalfopristin against antibiotic-resistant strains of haemophilus
666 influenzae, Staphylococcus aureus, and Streptococcus pneumoniae. Curr. Microbiol.
667 **51:**363-366.

668 10. **Politano AD, Sawyer RG.** 2010. NXL-103, a combination of flopristin and linopristin,
669 for the potential treatment of bacterial infections including community-acquired
670 pneumonia and MRSA. Curr. Opin. Investig. Drugs **11:**225-236.

AAC Accepts published online ahead of print

671 11. **Delgado G, Jr., Neuhauser MM, Bearden DT, Danziger LH.** 2000. Quinupristin-
672 dalfopristin: an overview. Pharmacotherapy **20:**1469-1485.

673 12. **Vazquez D.** 1966. Studies on the mode of action of the streptogramin antibiotics. J. Gen.
674 Microbiol. **42:**93-106.

675 13. **Bouanchaud DH.** 1992. In-vitro and in-vivo synergic activity and fractional inhibitory
676 concentration (FIC) of the components of a semisynthetic streptogramin, RP 59500. J.
677 Antimicrob. Chemother. **30 Suppl A:**95-99.

678 14. **Cocito C.** 1979. Antibiotics of the virginiamycin family, inhibitors which contain
679 synergistic components. Microbiol. Rev. **43:**145-192.

680 15. **Neu HC, Chin NX, Gu JW.** 1992. The in-vitro activity of new streptogramins, RP
681 59500, RP 57669 and RP 54476, alone and in combination. J. Antimicrob. Chemother. **30**
682 **Suppl A:**83-94.

683 16. **Chinali G, Nyssen E, Di Giambattista M, Cocito C.** 1988. Action of erythromycin and
684 virginiamycin S on polypeptide synthesis in cell-free systems. Biochim. Biophys. Acta
685 **951:**42-52.

686 17. **Chinali G, Nyssen E, Di Giambattista M, Cocito C.** 1988. Inhibition of polypeptide
687 synthesis in cell-free systems by virginiamycin S and erythromycin. Evidence for a
688 common mode of action of type B synergimycins and 14-membered macrolides.
689 Biochim. Biophys. Acta **949:**71-78.

690 18. **Pestka S.** 1977. p. 468-497, Moleculare Mechanisms of Protein Bioshnthesis. Academic
691 Press, New York.

AAC Accepts published online ahead of print

692 19. **Cocito C, Vanlinden F.** 1983. Inhibitory action of virginiamycin components on cell-
693 free systems for polypeptide formation from Bacillus subtilis. Arch. Microbiol. **135:**8-11.

694 20. **Contreras A, Vazquez D.** 1977. Synergistic interaction of the streptogramins with the
695 ribosome. Eur. J. Biochem. **74:**549-551.

696 21. **Parfait R, de Bethune MP, Cocito C.** 1978. A spectrofluorimetric study of the
697 interaction between virginiamycin S and bacterial ribosomes. Mol. Gen. Genet. **166:**45-
698 51.

699 22. **Hansen JL, Moore PB, Steitz TA.** 2003. Structures of five antibiotics bound at the
700 peptidyl transferase center of the large ribosomal subunit. J. Mol. Biol. **330:**1061-1075.

701 23. **Harms JM, Schlunzen F, Fucini P, Bartels H, Yonath A.** 2004. Alterations at the
702 peptidyl transferase centre of the ribosome induced by the synergistic action of the
703 streptogramins dalfopristin and quinupristin. BMC Biol. **2:**4.

704 24. **Tu D, Blaha G, Moore PB, Steitz TA.** 2005. Structures of MLSBK antibiotics bound to
705 mutated large ribosomal subunits provide a structural explanation for resistance. Cell
706 **121:**257-270.

707 25. **Hsieh MH, Yu CM, Yu VL, Chow JW.** 1993. Synergy assessed by checkerboard. A
708 critical analysis. Diagn. Microbiol. Infect. Dis. **16:**343-349.

709 26. **Schuwirth BS, Borovinskaya MA, Hau CW, Zhang W, Vila-Sanjurjo A, Holton JM,**
710 **Cate JH.** 2005. Structures of the bacterial ribosome at 3.5 A resolution. Science
711 **310:**827-834.

AAC Accepts published online ahead of print

27. **Zhang W, Dunkle JA, Cate JH.** 2009. Structures of the ribosome in intermediate states of ratcheting. Science **325:**1014-1017.

28. **Kabsch W.** 2010. XDS. Acta Crystallogr. D Biol. Crystallogr. **66:**125-132.

29. **Adams PD, Afonine PV, Bunkoczi G, Chen VB, Davis IW, Echols N, Headd JJ, Hung LW, Kapral GJ, Grosse-Kunstleve RW, McCoy AJ, Moriarty NW, Oeffner R, Read RJ, Richardson DC, Richardson JS, Terwilliger TC, Zwart PH.** 2010. PHENIX: a comprehensive Python-based system for macromolecular structure solution. Acta Crystallogr. D Biol. Crystallogr. **66:**213-221.

30. **Emsley P, Cowtan K.** 2004. Coot: model-building tools for molecular graphics. Acta Crystallogr. D Biol. Crystallogr. **60:**2126-2132.

31. **CLSI.** 2012. Methods for Dilution Antimicrobial Susceptibility Tests for Bacteria that Grow Aerobically; Approved Standard-Ninth Edition. CLSI document M07-A9. Wayne, PA.

32. **CLSI.** 2013. Performance Standards for Antimicrobial Susceptibility Testing; Twenty-Third Informational Supplement. CLSI document M100-S23. Wayne, PA.

33. **Pillai SK, Moellering RC, Jr., Eliopoulos GM.** 2005. Antimicrobial combinations, p. 365-440. *In* Lorian V (ed.), Antibiotics in Laboratory Medicine, 5th ed.

34. **Meletiadis J, Pournaras S, Roilides E, Walsh TJ.** 2010. Defining fractional inhibitory concentration index cutoffs for additive interactions based on self-drug additive combinations, Monte Carlo simulation analysis, and in vitro-in vivo correlation data for

antifungal drug combinations against Aspergillus fumigatus. Antimicrob. Agents Chemother. **54:**602-609.

35. **Odds FC.** 2003. Synergy, antagonism, and what the chequerboard puts between them. J. Antimicrob. Chemother. **52:**1.

36. **Brosius J, Ullrich A, Raker MA, Gray A, Dull TJ, Gutell RR, Noller HF.** 1981. Construction and fine mapping of recombinant plasmids containing the rrnB ribosomal RNA operon of E. coli. Plasmid **6:**112-118.

37. **Buurman ET, Foulk MA, Gao N, Laganas VA, McKinney DC, Moustakas DT, Rose JA, Shapiro AB, Fleming PR.** 2012. Novel rapidly diversifiable antimicrobial RNA polymerase switch region inhibitors with confirmed mode of action in Haemophilus influenzae. J. Bacteriol. **194:**5504-5512.

38. **Pankuch GA, Kelly LM, Lin G, Bryskier A, Couturier C, Jacobs MR, Appelbaum PC.** 2003. Activities of a new oral streptogramin, XRP 2868, compared to those of other agents against Streptococcus pneumoniae and haemophilus species. Antimicrob. Agents Chemother. **47:**3270-3274.

39. **Mukhtar TA, Wright GD.** 2005. Streptogramins, oxazolidinones, and other inhibitors of bacterial protein synthesis. Chem. Rev. **105:**529-542.

40. **Depardieu F, Courvalin P.** 2001. Mutation in 23S rRNA responsible for resistance to 16-membered macrolides and streptogramins in Streptococcus pneumoniae. Antimicrob. Agents Chemother. **45:**319-323.

AAC Accepts published online ahead of print

752 41. **Wang G, Taylor DE.** 1998. Site-specific mutations in the 23S rRNA gene of
753 Helicobacter pylori confer two types of resistance to macrolide-lincosamide-
754 streptogramin B antibiotics. Antimicrob. Agents Chemother. **42:**1952-1958.

755 42. **Sigmund CD, Ettayebi M, Morgan EA.** 1984. Antibiotic resistance mutations in 16S
756 and 23S ribosomal RNA genes of Escherichia coli. Nucleic Acids Res. **12:**4653-4663.

757 43. **Cocito C, Di Giambattista M, Nyssen E, Vannuffel P.** 1997. Inhibition of protein
758 synthesis by streptogramins and related antibiotics. J. Antimicrob. Chemother. **39 Suppl**
759 **A:**7-13.

760 44. **Singh KV, Weinstock GM, Murray BE.** 2002. An Enterococcus faecalis ABC
761 homologue (Lsa) is required for the resistance of this species to clindamycin and
762 quinupristin-dalfopristin. Antimicrob. Agents Chemother. **46:**1845-1850.

763 45. **Ban N, Nissen P, Hansen J, Moore PB, Steitz TA.** 2000. The complete atomic structure
764 of the large ribosomal subunit at 2.4 A resolution. Science **289:**905-920.

765 46. **Churchill CD, Navarro-Whyte L, Rutledge LR, Wetmore SD.** 2009. Effects of the
766 biological backbone on DNA-protein stacking interactions. Phys. Chem. Chem. Phys.
767 **11:**10657-10670.

768

769

770 FIGURE LEGENDS

771

772 **FIG 1.** Structures of streptogramins bound to the *E. coli* 70S ribosome. A) Cross section through
773 the bacterial 50S subunit with the peptidyl-transferase center (PTC) and the exit tunnel labeled.

AAC Accepts published online ahead of print

AAC Accepts published online ahead of print

774 Streptogramin A (yellow) and streptogramin B (green) are shown. B) Chemical structure of
775 streptogramin antibiotics with differences indicated in red. C) and D) Unbiased F_{obs}-F_{calc}
776 difference density shown as mesh with chemical structure of Synercid and NXL 103,
777 respectively. Residue A2062 in the vacant 70S ribosome is shown in transparent green. E)
778 U2585 assumes different positions in the vacant 70S ribosome (green), and the 70S ribosome in
779 complex with either NXL 103 (cyan), and Synercid (salmon). Adjacent nucleotides, the
780 flopristin, and the dalfopristin component are shown by lines. The asterisk indicates the position
781 of U2585 when bound to dalfopristin under hydrolytic conditions. F) Conformational changes
782 between the vacant ribosome (green) and the NXL 103 bound ribosome (cyan) are shown.
783 Identical changes are observed in the structure of dalfopristin under hydrolyzing conditions. G)
784 Interaction of linopristin (cyan) and quinupristin (salmon) with K90 of ribosomal protein L22. C)
785 - G) Hydrogen bonds are indicated by red dashed lines. Hydrogen bonds in the vacant ribosome
786 in F) are shown by green dashed lines.

787

788 **FIG 2.** Activity of different streptogramin combinations, for wild type and mutant 70S
789 ribosomes. A) Sequence alignment of 23S rRNA from various Gram-positive and Gram-negative
790 pathogens. Nucleotides 1782 and 2586 (shaded in red) form a base pair (Fig. S5,6). B-H) IC50
791 values in μM for different streptogramin antibiotics determined in transcription-coupled
792 translation assays from *E. coli* bearing either its intrinsic U-U base pair (B, C, E, and F) at
793 position 1782-2586 or a C-C base pair (B, D, G, and H). C and D) Comparison of IC50 values of
794 streptogramin A components in transcription-coupled translation assays either alone or in the
795 presence of streptogramin B at its IC50. E-H) Comparison of IC50 values of streptogramin B
796 components in transcription-coupled translation assays either alone or in the presence of various

797 streptogramin A components at their IC50 value. The standard deviation of the IC50 values,
798 measured in triplicate, is indicated by the error bars.

799

800

801

AAC Accepts published online ahead of print

AAC Accepts published online ahead of print

802 **Table 1**. Antimicrobial activity of different streptogramin antibiotics[a]

streptogramin	type[b]	*E. coli*[c]	*H. influenzae*[d]	*E. faecalis*[e]	*S. aureus*[f]	*S. pneumoniae*[g]
dalfopristin	A	4	1	64	4	4
quinupristin	B	>64	32	8	4	1
flopristin	A	1	0.25	64	1	2
linopristin	B	>64	>64	8	32	4
hydrolyzed dalfopristin	A	4	2	32	4	4
virginiamycin M	A	4	4	>64	8	8
Synercid	A+B	8	8	4	0.25	0.25
NXL 103	A+B	2	0.5	1	0.125	0.125

803

804 [a]Minimal Inihibitory Concentrations (MIC) were determined by the broth microdilution

805 technique and are given in µg/mL.

806 [b]Streptogramin type A or B or combination of A+B. Note that the A+B combinations are

807 formulated in a ratio of A:B of 70:30 (w/w).

808 [c]*E. coli* ATCC 29417 (MRE600), [d]*H. influenzae* ATCC 49247, [e]*E. faecalis* ATCC 29212, [f]*S.*

809 *aureus ATCC* 29213, [g]*S. pneumoniae* ATCC 49619

810

AAC Accepts published online ahead of print

811 **Table 2.** "Checkerboard" analysis to detect synergy

	E. faecalis[a]		*S. aureus*[b]	
streptogramin	dalfopristin / quinupristin (Synercid)	flopristin / linopristin (NXL 103)	dalfopristin / quinupristin (Synercid)	flopristin / linopristin (NXL 103)
FIC index range	0.25 to 4.0	0.05 to 4.0	0.05 to 4.0	0.03 to 1.0
Ø FIC index[c]	0.99	0.81	0.82	0.22
Ø FIC index[d]	0.3	0.1	0.12	0.08
synergistic combinations A / B[e]	16 / 0.5 8 / 1 4 / 2	4 / 0.06 2 / 0.125 1 / 0.25 0.5 / 0.5 0.25 / 1 0.125 / 2	0.5 / 0.06 0.125 / 0.125 0.125 / 0.25 0.06 / 0.5 0.06 / 1 0.06 / 2	0.06 / 0.06 0.06 / 0.125 0.06 / 0.25 0.03 / 0.5 0.03 / 1 0.015 / 2 0.015 / 4 0.015 / 8

812

813 [a]*E. faecalis* ATCC 29212 and [b]*S. aureus* ATCC 29213

814 [c]Ø FIC index = mean Fractional Inhibitory Concentration index for all combinations.

815 [d]Ø FIC index = mean Fractional Inhibitory Concentration index for all combinations that lead to

816 synergy.

817 [e]Concentration of streptogramin A and streptogramin B in µg/mL that lead to synergy.

818 **Table 3.** Determination of streptogramin affinity for 70S ribosomes by isothermal titration
819 calorimetry (ITC)

cell content	injectant	dissociation constant (K_d)[a]
70S	quinupristin	44 ± 21
70S + dalfopristin[b]	quinupristin	7 ± 5
70S	linopristin	40 ± 6
70S + flopristin[c]	linopristin	12 ± 8

820

821 [a]Values are given in nM and are the average of three independent experiments with their
822 standard deviations indicated.

823 70S ribosomes were either pre-bound to dalfopristin[b] or flopristin[c].

AAC Accepts published online ahead of print

AAC Accepts published online ahead of print

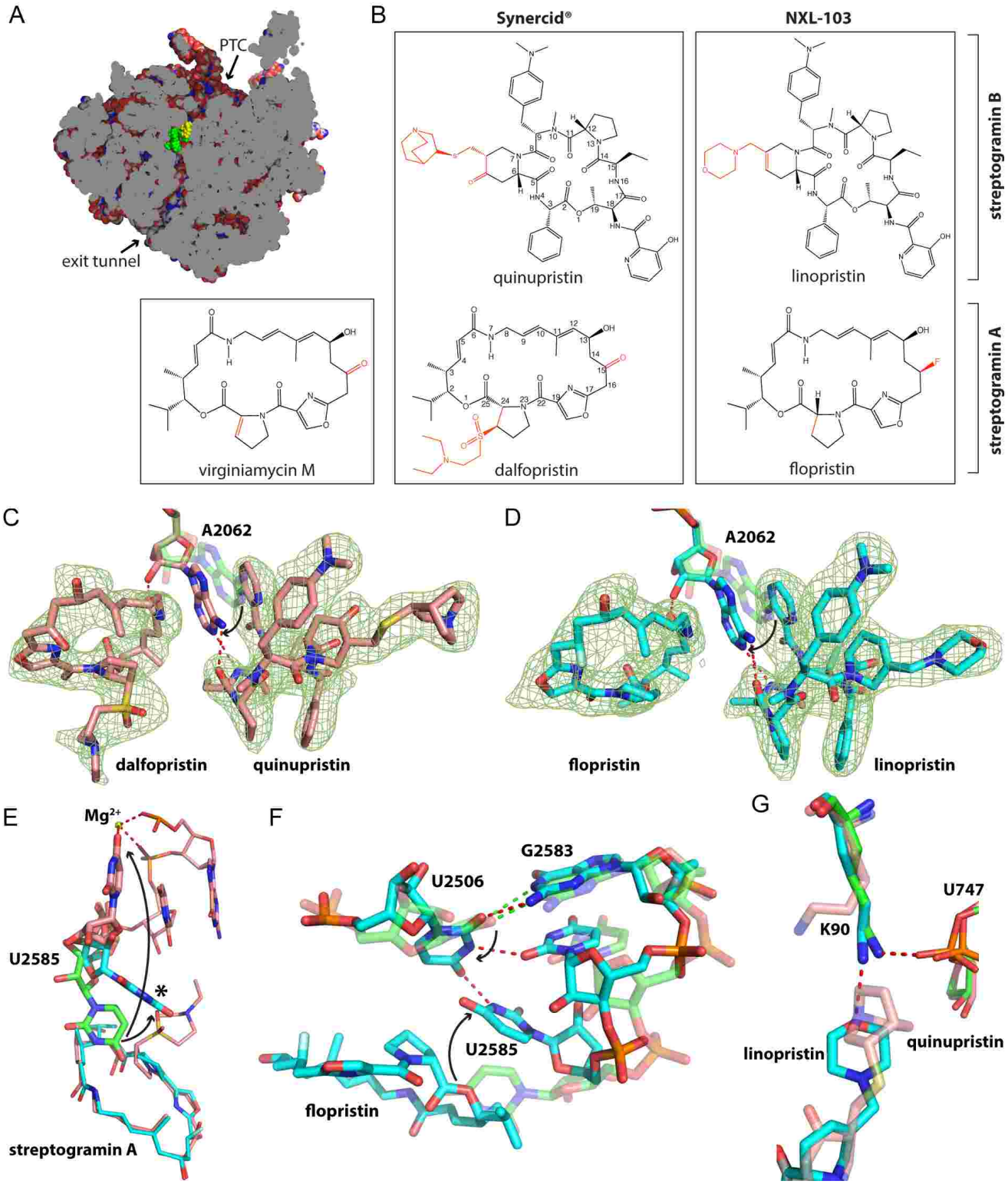

AAC Accepts published online ahead of print

A

	1782	2586	Gram stain
Bacillus_subtilis	UAGCAAA ·····	GUUCAGA	+
Bacillus_anthracis	UAGCAAA ·····	GUUCAGA	+
Listeria_monocytogenes	UAGCAAA ·····	GUUCAGA	+
Staphylococcus_aureus	UAUCAAA ·····	GUUCAGA	+
Streptococcus_pneumoniae	UAUCAAA ·····	GUUCAGA	+
Streptococcus_pyogenes	UAUCAAA ·····	GUUCAGA	+
Enterococcus_faecalis	UAUCAAA ·····	GUUCAGA	+
Enterococcus_faecium	UAUCAAA ·····	GUUCAGA	+
Lactobacillus_plantarum	UAUCAAA ·····	GUUCAGA	+
Clostridium_difficile	UACCAAA ·····	GUUCAGA	+
Propionibacterium_avidum	UACCAAA ·····	GUUCAGA	+
Escherichia_coli	UAUUAAA ·····	GUUUAGA	-
Klebsiella_pneumoniae	UAUUAAA ·····	GUUUAGA	-
Vibrio_cholerae	UAUUAAA ·····	GUUUAGA	-
Haemophilus_influenzae	UAUUAAA ·····	GUUUAGA	-
Moraxella_catarrhalis	UAUUAAA ·····	GUUUAGA	-
Pseudomonas_aeruginosa	UAUUAAA ·····	GUUUAGA	-
Legionella_pneumophilia	UAUUAAA ·····	GUUUAGA	-
	** ***	*** ***	

B

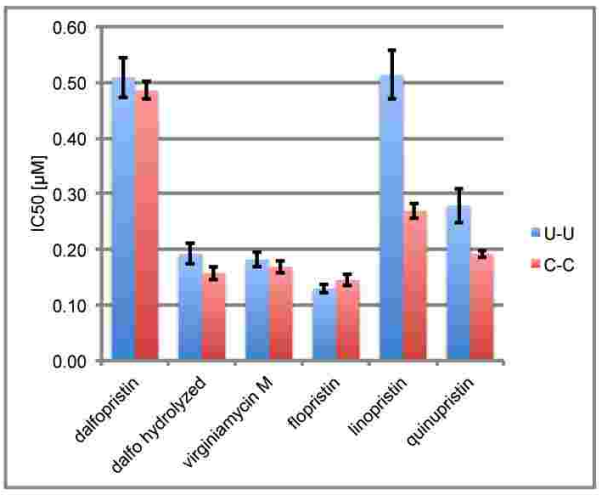

C

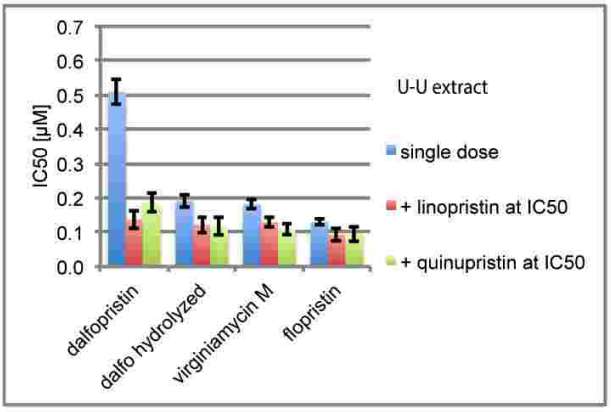

D

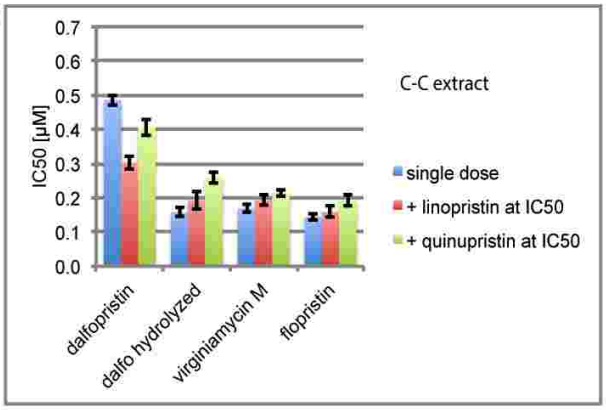

E

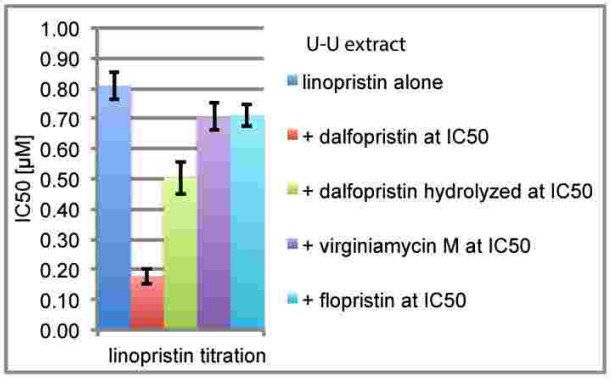

F

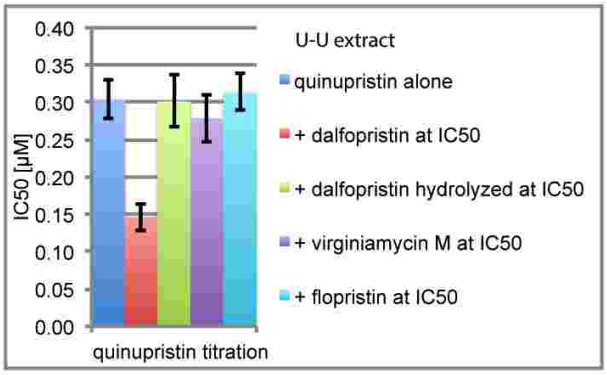

G

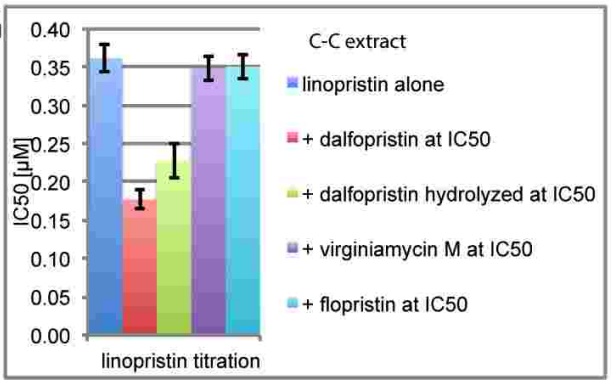

H